J Stomatol Oral Maxillofac Surg 000 (2024) 101936

Available online at ScienceDirect www.sciencedirect.com

Elsevier Masson France EM|consulte www.em-consulte.com

Original Article

Effects of different expansion appliances and surgical incisions on maxillary expansion: A finite element analysis

Ece Mersan Ateş[a], Hande Pamukçu[a,*], Osman Koç[b], Nur Altıparmak[c]

[a] Department of Orthodontics, School of Dentistry, Baskent University, Ankara, Turkey
[b] Faculty of Mechanical Engineering, Yildiz Technical University, Istanbul, Turkey
[c] Department of Oral and Maxillofacial Surgery, School of Dentistry, Baskent University, Ankara, Turkey

ARTICLE INFO

Article History:
Received 3 April 2024
Accepted 2 June 2024
Available online xxx

Keywords:
Finite element analysis
Rapid palatal expansion
Palatal expansion techniques

ABSTRACT

Purpose: This study aims to assess the impact of different surgical techniques and three expansion appliances on maxillary expansion in adults using finite element analysis (FEA), with a focus on maxillary displacement and stress on surrounding structures.
Methods: Seven different FEA models were created to compare different surgical techniques and three different expansion appliances. Model I represented a bone-supported appliance without surgical assistance. Model II, Model III, and Model IV were surgically assisted rapid palatal expansion (SARPE) models without pterygomaxillary suture disjunction (PMD). Model V, Model VI, and Model VII were SARPE models with PMD.
Results: The largest displacement at the anterior nasal spine (ANS) was recorded for Model II (2.95 mm). For the posterior nasal spine (PNS), the highest displacement was observed in Models V, VI, VII (2.50 mm), with the lowest in Model III (0.79 mm). Stress analysis revealed the highest stress in Model I, with models featuring PMD displaying nearly zero stress at all anatomical points, highlighting distinct expansion patterns and stress distributions between models with and without PMD.
Conclusion: SARPE models with PMD demonstrated a parallel expansion of the maxilla with minimal stress, while the miniscrew assisted rapid maxillary expansion (MARPE) model displayed transverse rotation. SARPE models without PMD exhibited a V-shaped expansion pattern. SARPE models with PMD represent an optimal approach for achieving uniform expansion and minimizing stress, with stress levels nearly negligible at all anatomical points in models with PMD.
© 2024 Elsevier Masson SAS. All rights are reserved, including those for text and data mining, AI training, and similar technologies.

1. Introduction

Rapid maxillary expansion in growing patients involves applying a force that exceeds physiological limits in the transverse direction to the dentoalveolar structures leading to the separation of the median palatal suture and the transverse expansion of the upper jaw [1]. In adult patients, due to fusion of the maxillary suture and in order to prevent side effects, palatal expansion could be accompanied by a partial maxillary osteotomy at the LeFort I level, a procedure known as surgically assisted rapid palatal expansion (SARPE) [2]. Different osteotomies could be performed for SARPE. However, a consensus on the minimum surgical technique has not yet been established in the existing literature, and it varies according to surgeons' training and preferences [3]. Divergent viewpoints exist, with some advocating for a comprehensive disjunction of all maxillary resistance areas, involving sequential pterygoid and midpalatal osteotomies, followed by paramedian osteotomies. Conversely, other studies argue that pterygomaxillary suture disjunction (PMD) is unnecessary. They claim that both techniques are reliable to achieve maxillary expansion, with minor variations in skeletal and dental changes. SARPE with PMD does not entirely eliminate all posterior bone resistance but rather facilitates bone movement. Some studies suggested that this technique supports more substantial expansion of the posterior palatal region, especially in severe skeletal posterior crossbite cases requiring extensive expansion [4]. Nevertheless, SARPE may lead to complications, incurring additional time and financial costs. SARPE without PMD showed an increased occurrence of minor complications (29.95% vs. 16.87 %) [5]. A systematic review indicated a lack of sufficient information in the existing literature regarding the outcomes of SARPE with PMD. Consequently, the authors emphasized the need for further research in this area [6].

In recent years, miniscrew-assisted rapid palatal expansion (MARPE) has gained popularity as a potential alternative to SARPE [7]. The utilization of orthodontic miniscrews has facilitated the

* Corresponding author at: Başkent Üniversitesi Diş Hekimliği Fakültesi, Ortodonti Anabilim Dalı, 11.sok, No:26, 06490 Bahçelievler, ANKARA, Türkiye.
E-mail address: hpamukcu@baskent.edu.tr (H. Pamukçu).

https://doi.org/10.1016/j.jormas.2024.101936
2468-7855/© 2024 Elsevier Masson SAS. All rights are reserved, including those for text and data mining, AI training, and similar technologies.

Please cite this article as: E.M. Ateş, H. Pamukçu, O. Koç et al., Effects of different expansion appliances and surgical incisions on maxillary expansion: A finite element analysis, Journal of Stomatology oral and Maxillofacial Surgery (2024), https://doi.org/10.1016/j.jormas.2024.101936

different designs of maxillary expansion devices that can produce skeletal maxillary expansion while minimizing undesirable effects on the teeth [8]. A recent study demonstrated that MARPE is an effective treatment approach for expanding the maxilla, with a mean success rate of 92.5 %, and MARPE leads to both skeletal (2.33 mm) and dental (6.55 mm) transverse maxillary expansion. These outcomes are clinically similar to the expansion achieved through SARPE [9]. Additionally, there is limited evidence suggesting that despite its relatively short treatment duration, MARPE may result in dental and periodontal side effects and have an impact on perioral soft tissues [10].

Numerous studies in the literature have used finite element analysis (FEA) to examine the displacement and stress on tissues like craniofacial structures, teeth, and the periodontal ligament (PDL) during simulations of mechanical orthodontic movements [11-16]. This approach allows for a detailed investigation into the biomechanical effects of procedures like MARPE and SARPE, providing insights into the distribution of stress and deformation within these biological tissues. FEA contributes significantly to the optimization of treatments, aiding in better treatment planning and mitigating potential adverse effects.

This study aimed to assess the impact of different surgical techniques (MARPE, SARPE with/without PMD) and three distinct expansion appliances on maxillary expansion in adult patients, utilizing finite element analysis. This study also aimed to assess the amount of displacement in the maxilla and the amount of stress exerted on surrounding structures. The null hypothesis of this study is that there will be no difference in the effects of various surgical techniques and different types of expansion appliances on maxillary expansion.

2. Materials and methods

This study was approved by Başkent University Institutional Review Board (Project no. D-KA23/02) and supported by Başkent University Research Fund.

The (MRI) anatomical model of an adult male skull was downloaded in .stl format as a part of the open-source BodyParts3D project (The skull bones, including frontal, parietal, sphenoid, ethmoid, nasal, lacrimal, zygomatic, and occipital bones, were integrated into the same coordinate system using Ansys Workbench 19.3 (ANSYS Inc., Houston, PA, USA) software in .stl format [17]. (https://dbarchive.biosciencedbc.jp/jp/bodyparts3d/desc.html)

The FEA model utilized similarities with the previous skull bone models, with distinctions in miniscrew locations and the inclusion of miniscrew thread for a comprehensive examination of cranial structures [14-16]. A general skull bone model was created; the periodontal ligament (0.2 mm) and the midpalatal suture (0.25 mm) were modeled using the offset command, depending on the tooth and maxilla geometry, respectively. The midpalatal suture was included in the central part of the maxilla. The maxilla, midpalatal suture (for a single model), tooth and PDL were included in the overall model independently (Figs. 1 and 2). Ansys SpaceClaim software was used to design three types of expanders and miniscrews; bone-supported, tooth-bone-supported, and digitally designed tooth-supported. To ensure standardization, miniscrews of the same length and diameter (1.6 mm in diameter; 12 mm in length) were used in all miniscrew-supported models [15]. Designed expansion appliances and miniscrews were included in the models (Fig. 2). Cortical bone, cancellous bone, and PDL were considered anisotropic materials. Conversely, the tooth, midpalatal suture, and stainless steel were assumed to be homogeneous and isotropic [14-16]. A hyper-elastic material model (third-order Ogden) was utilized for defining the PDL. The material properties for each component were detailed in Table 1.

For FEA, a symmetrical model of the craniofacial and maxillofacial structures was created, as shown in Fig. 1. Seven different models were created to compare the FEA scenario results. The models were created based on the type of expansion appliance used, the presence of surgical assistance, and the SARPE procedure with or without PMD (Fig. 2, Table 2).

In Model I, without any surgical assistance, miniscrews of the bone-supported appliance were placed 3 mm distal to the median

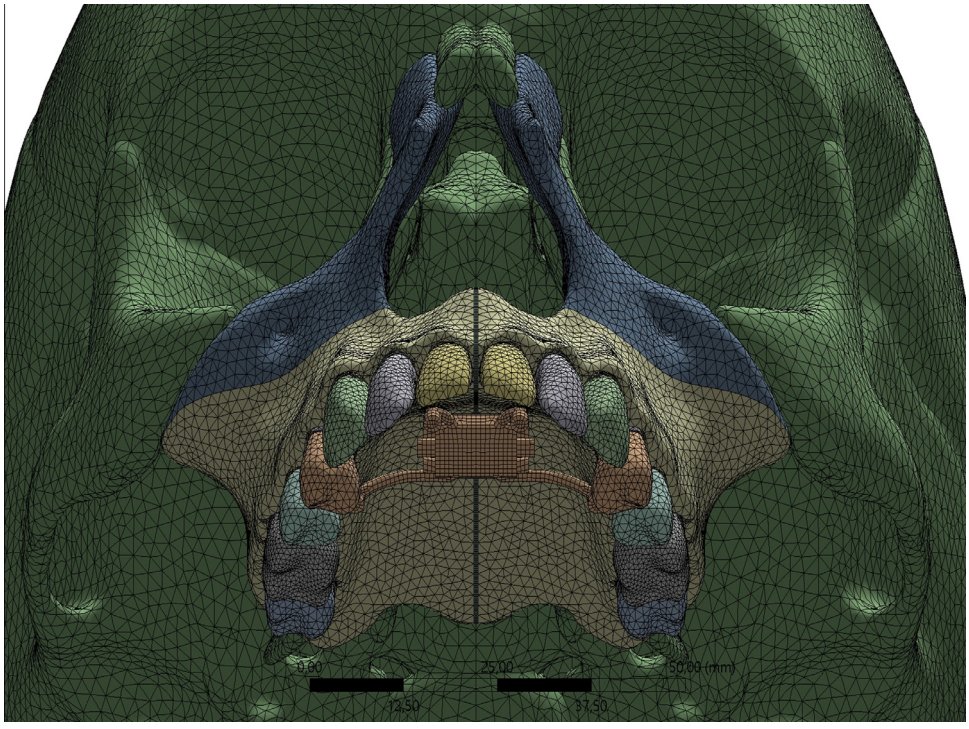


Fig. 1. A symmetric model of craniofacial and maxillofacial structures and the mesh structure of the whole model. Frontal view of the model divided into 10-node quadratic tetrahedral and 20-node quadratic hexahedral mesh element types.

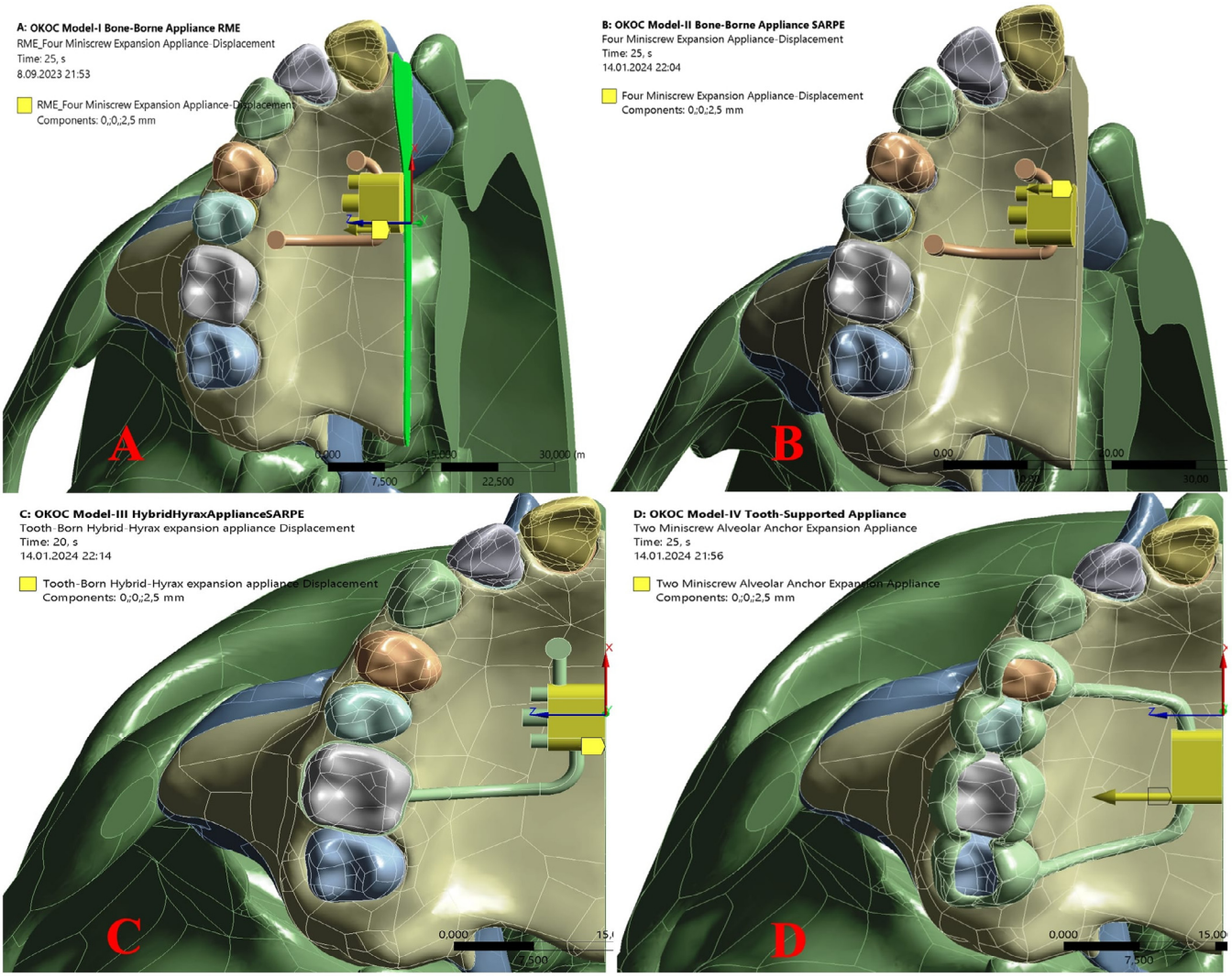


Fig. 2. A, In Model I, without any surgical assistance, miniscrews of the bone-supported appliance were placed 3 mm distal to the median suture at the level of the 3rd rugae and 6 mm from the alveolar crest between the roots of the 2nd premolar and 1st molar teeth; **B,** median and lateral osteotomies were performed, without pterygomaxillary suture disjunction (PMD). Miniscrews of the expansion appliance were placed at the same site as in Model I; **C,** Median and lateral osteotomies were performed without PMD. The expansion appliance miniscrew was placed 3 mm distal to the median suture at the level of the 3rd rugae. A molar band was placed on the first molar and a modified hybrid Hyrax appliance was created. **D,** median and lateral osteotomies were performed without PMD. A digitally designed tooth-supported appliance was created, featuring a 1 mm thick stainless-steel casting covering the 1st premolar, 2nd premolar, 1st molar, and 2nd molar, along with a centrally positioned Hyrax expansion screw.
The 2.5 mm transversal displacement movement (total 5 mm) of the expansion appliance, indicated by yellow arrows.

Table 1
Finite element model's material properties.

Material properties (Mpa)	Elastic modulus	Poisson's ratio	Shear modulus
Cortical Maxillary bone	Ex:12,000	Vxy: 0.18	Gxy: 3600
	Ey: 11,640	Vyz: 0.40	Gyz: 5400
	Ez: 15,600	Vxz: 0.30	Gxz: 4100
Cortical Skull bone	Ex: 12,580	Vxy: 0.48	Gxy: 4400
	Ey: 13,600	Vyz: 0.24	Gyz: 6700
	Ez: 21,200	Vxz: 0.32	Gxz: 4900
Cancellous bone	Ex:1448	Vxy: 0.32	Gxy: 434
	Ey: 1448	Vyz: 0.05	Gyz: 68
	Ez: 210	Vxz: 0.05	Gxz: 68
Periodontal Ligament	$\mu_{1:}$ - 3420.83	$\mu_{2:}$ 1434.35	$\mu_{3:}$ - 5.56E-04
	$\alpha_{1:}$ - 0.506	$\alpha_{2:}$ - 0.134	$\alpha_{3:}$ 13.708
	$D_{1:}$ 0 MPa^{-1}	$D_{2:}$ 0 MPa^{-1}	$D_{3:}$ 0 MPa^{-1}
Dentin	19,890	0.31	
Midpalatal Suture	0.69	0.45	
Stainless steel	193,000	0.35	

MPa: Megapascal.
Ex, Ey, Ez: Elastic modulus in three directions.
Vxz, Vyz, Vxz: Poisson's ratio in three directions.
Gxy, Gyz, Gxz: Shear modulus in three directions.
μ, α, D : Material parameters.

suture at the level of the 3rd rugae and 6 mm from the alveolar crest between the roots of the 2nd premolar and 1st molar teeth (Fig. 2.A, Table 2).

In Model II, median and lateral osteotomies were performed, without PMD. Miniscrews of the expansion appliance were placed at the same site as in Model-I (Fig. 2.B, Table 2).

Table 2
Comparison of the study models.

	Appliance type	SARPE or MARPE	Pterygomaxillary Suture Disjunction(PMD)
Model I	Bone-borne	MARPE	–
Model II	Bone-borne	SARPE	–
Model III	Hybrid-hyrax	SARPE	–
Model IV	Tooth-supported	SARPE	–
Model V	Bone-borne	SARPE	+
Model VI	Hybrid-hyrax	SARPE	+
Model VII	Tooth-supported	SARPE	+

Table 3
Finite element model's element, nodes, mesh size and average skewness element quality convergence values.

	Average skewness value	Nodes	Element	Mesh size (milimeters)	Mesh Element Type
Skull	0.15	1,691,902	1,158,657	1.8	Tetrahedral
Maxilla (lower part)	0.28	209,146	142,883	1.3	Tetrahedral
Maxilla (upper part)	0.15	104,642	71,184	1.3	Tetrahedral
Periodontal ligament	0.4	95,057	47,053	0.6	Tetrahedral
Suture	0.08	38,637	6752	0.3	Hex dominant
Tooth	0.18	159,921	106,775	0.8	Tetrahedral
Tooth supported (hyrax) palatal expander	0.63	34,744	11,014	0.6	Hexahedral
Tooth supported (Digital) palatal expander	0.67	59,485	21,461	0.6	Hexahedral
Tooth-bone-borne palatal expander	0.63	59,160	19,365	0.6	Hexahedral

In Model III, median and lateral osteotomies were performed without PMD. The expansion appliance miniscrew was placed 3 mm distal to the median suture at the level of the 3rd rugae. A molar band was placed on the first molar and a modified hybrid Hyrax appliance was created (Fig. 2.C, Table 2).

In Model IV, median and lateral osteotomies were performed without PMD. A digitally designed tooth-supported model was created, featuring a 1 mm thick stainless-steel casting covering the 1st premolar, 2nd premolar, 1st molar, and 2nd molar, along with a centrally positioned Hyrax expansion screw (Fig. 2.D, Table 2).

In Model V, median, lateral osteotomies and PMD were performed. Four miniscrews of the expansion appliance were placed at the same site as in Model I (Table 2).

In Model VI, median, lateral osteotomies and PMD separation were performed. A hybrid Hyrax expansion appliance model was created similar to Model III (Table 2).

In Model VII, median, lateral osteotomies and PMD were performed. A digitally designed tooth-supported model was created similar to Model I (Table 2).

Table 4
The unilateral displacements (mm) based on the direction after 5 mm of activation of palatal expander in all models.

	Model-I			Model-II			Model-III			Model-IV		
Anatomical structure	X	Y	Z	X	Y	Z	X	Y	Z	X	Y	Z
Central incisor	0.503	0.407	3.240	0.178	-0.087	3.509	0.232	-0.355	3.318	0.090	-1.576	3.344
Lateral incisor	0.455	0.804	3.350	-0.028	0.031	3.381	0.043	-0.242	3.199	-0.008	-1.219	3.268
Canine	0.369	1.090	3.190	-0.264	0.146	3.149	-0.189	-0.092	2.964	-0.125	-0.853	3.043
First premolar	0.309	1.156	2.929	-0.384	0.233	2.806	-0.317	-0.009	2.598	-0.195	-0.550	2.734
Second premolar	0.261	1.179	2.690	-0.547	0.311	2.535	-0.484	0.098	2.295	-0.323	-0.291	2.542
First molar	0.106	1.135	2.354	-0.508	0.398	2.212	-0.450	0.216	2.030	-0.293	0.005	2.312
Second molar	0.028	1.032	1.916	-0.435	0.411	1.667	-0.369	0.246	1.440	-0.209	0.165	1.914
Anterior nasal spine	0.199	-0.092	1.784	0.304	-0.167	2.950	0.372	-0.473	2.710	0.203	-1.856	2.150
Posterior nasal spine	0.310	-0.271	1.230	0.399	-0.098	0.983	0.446	-0.155	0.798	0.230	-0.945	1.080
Frontomaxillary suture	-0.426	0.740	0.006	-0.261	0.399	0.000	-0.169	0.231	0.003	-0.085	0.195	0.000
Zygomaticomaxillary suture	-0.293	1.469	0.922	-0.087	0.047	0.058	-0.070	0.264	0.048	0.069	0.286	0.095
Frontozygomatic suture	-0.720	1.134	0.108	-0.282	0.399	0.011	-0.179	0.229	0.007	-0.127	0.211	0.017
Zygomatic arch	-0.461	0.772	0.553	-0.128	0.273	0.031	-0.097	0.151	0.028	-0.048	0.105	-0.002
Medial pterygoid plate	-0.185	0.696	0.802	-0.438	0.341	0.385	-0.370	0.206	0.281	-0.162	0.174	0.385
Lateral pterygoid plate	-0.160	0.519	0.661	-0.259	0.353	0.202	-0.234	0.263	0.156	-0.113	0.189	0.274
Angle of rotation and tipping	1.04°	-3.58°	-0.87°	0.10°	1.65°	-2.8°	0.44°	1.91°	-2.76°	1.29°	1.96°	-1.66°

	Model-V			Model-VI			Model-VII		
Anatomical structure	X	Y	Z	X	Y	Z	X	Y	Z
Central incisor	0.0001	0.0000	2.500	0.0000	0.0000	2.500	-0.0000	0.0001	2.500
Lateral incisor	-0.0000	-0.0000	2.500	0.0000	0.0000	2.500	-0.0000	0.0000	2.500
Canine	-0.0003	-0.0000	2.500	0.0000	0.0000	2.500	0.0000	-0.0000	2.500
First premolar	-0.0004	-0.0000	2.500	0.0000	0.0000	2.500	0.0000	-0.0000	2.500
Second premolar	-0.0006	-0.0000	2.500	0.0000	-0.0000	2.500	0.0000	-0.0000	2.500
First molar	-0.0005	-0.0000	2.500	0.0000	-0.0000	2.500	0.0000	-0.0000	2.500
Second molar	-0.0006	-0.0000	2.500	0.0000	-0.0000	2.500	0.0000	0.0001	2.500
Anterior nasal spine	0.0002	0.0000	2.500	-0.0000	0.0000	2.500	-0.0000	0.0001	2.500
Posterior nasal spine	0.0002	0.0000	2.500	-0.0000	-0.0000	2.500	-0.0000	0.0000	2.500
Frontomaxillary suture	-0.0000	0.0000	1.8e-9	0.0000	-0.0000	1.9e-7	-0.0000	0.0000	1.2e-6
Zygomaticomaxillary suture	0.0000	0.0000	1.6e-6	0.0000	0.0000	1.6e-5	0.0000	0.0000	3.5e-6
Frontozygomatic suture	-0.0000	0.0000	5.1e-8	-0.0000	-0.0000	1.1e-6	-0.0000	0.0000	8.5e-8
Zygomatic arch	-0.0000	0.0000	3.3e-7	0.0000	-0.0000	-1.3e-6	-0.0000	0.0000	5.1e-7
Medial pterygoid plate	0.0000	0.0000	-1.8e-7	0.0001	0.0000	1.8e-5	0.0000	0.0000	2.1e-6
Lateral pterygoid plate	0.0000	0.0000	-9.6e-8	0.0000	-0.0000	-1.9e-5	0.0000	0.0000	9.9e-7
Angle of rotation and tipping	$-5.8e^{-5}$ °	$-1e^{-3}$ °	$-2.5e^{-3}$°	1.6e-4°	-4.1e-4°	6.4e-4°	-1.9e-6°	-8.8e-5°	5.2e-5°

Note: x, x-axis (anteroposterior); y, y-axis (longitudinal or vertical); z, z-axis (transverse dimensions).
Positive (+) values indicate forward, outward or upward displacement, and negative (−) values indicate backward, inward or downward displacement.
Median and lateral osteotomies were made in all models without pterygomaxillary suture separation.
'e': Exponential. 'e' signifies the representation of a number as a base raised to a power/exponent.
10 to the power is expressed as a negative or positive (-/+) number.

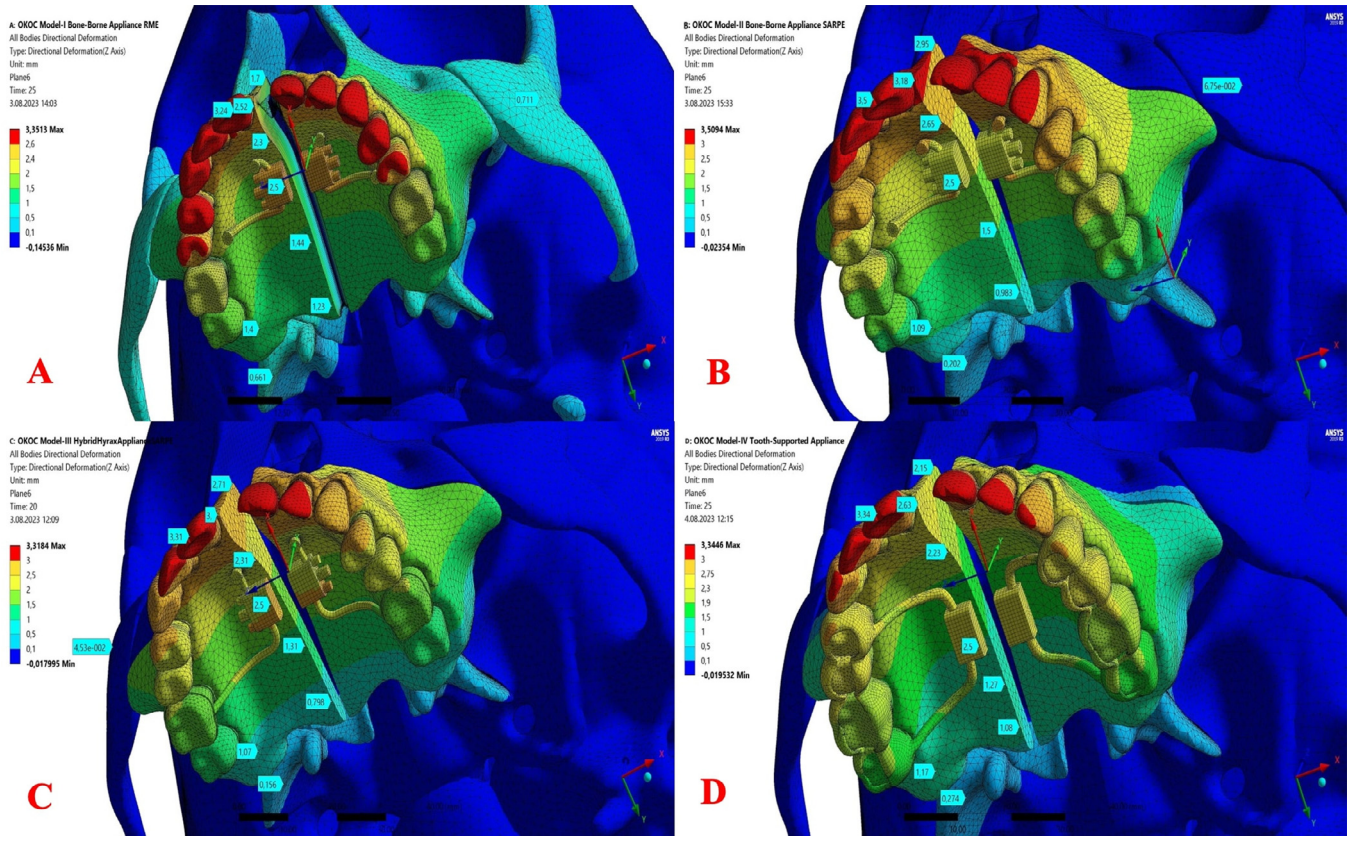


Fig. 3. **A**, Model I; **B**, Model II; **C,** Model III; **D,** Model-IV; **E,** Model-V; **F,** Model-VI; **G,** Model-VII; showing the amount of displacement (in mm) in the z-axis (occlusal perspective).

2.1. Boundary conditions

The coordinates have been defined using the anterior-posterior axis as the x-axis, the longitudinal or vertical axis as the y-axis, and the transverse axis as the z-axis. Each state of deformation and stress value is displayed using a distinct color scale band. In the models, elemental von Mises stress values were measured in MPa and displacement values were measured in mm. Transient structural analysis (dynamic analysis) was used to evaluate the displacement and von Mises stress distribution. Geometric nonlinear theory, nonlinear contact theory and nonlinear material methods were considered. Displacement and stress values were measured using a probe on the same element across all models in ANSYS Workbench software.

The foramen magnum was fixed to serve as the origin [11]. Displacement movement was transmitted to the maxilla via miniscrews, and the expansion screw was activated at 0.25 mm in all models. In the symmetrical FEA model, a transverse displacement of 2.5 mm was given, equivalent to a 5 mm movement along the z-axis. The results were measured following a total activation of 5 mm simulating a scenario representative of clinical conditions.

In all models, a frictionless contact was defined between the maxillary surfaces separated by lateral osteotomy. Bonded contacts were established between the maxilla and teeth, PDL, and screws of the expansion appliance. They functioned as a single unit; no sliding or separation between faces and edges were permitted. In models with PMD (between the maxilla and the sphenoid bone), friction contact was defined between the contacting surfaces (friction coefficient of 0.3). Separation or sliding of contacting surfaces and edges is allowed.

The amount of rotation for the maxilla was gauged by observing the angular changes along the line passing through nodes between the anterior nasal spine (ANS)-posterior nasal spine (PNS) points concerning the skull's symmetrical plane.

2.2. Finite element model

The bones of the skull were divided into elements with dimensions of 1.8 mm, the maxilla into 1.3 mm, the periodontal ligament into 0.6 mm, and the teeth into 1 mm. The elements were of type 10-node, quadratic tetrahedral. The expansion appliance and miniscrew were segmented into 0.6 mm, the midpalatal suture at 0.3 mm and 20-node, quadratic hexahedral mesh elements (Fig. 1). The element, node, and mesh size values were approximately the same for all models, with an average mesh skewness element quality convergence value of excellent (0,25) (Table 3). Previous FEA studies have shown the range of values (excellent-unacceptable) that indicate the quality of the skew mesh metric spectrum determined by the Ansys software [14-16] (Fig. 1). Table 3 shows the number of elements and nodes, mesh size values and element quality convergence range for all components of the models. The process of mesh convergence was carried out on the contact surfaces of the maxilla and sphenoid bone, miniscrew, the body of the first molar tooth, and the area where the anchorage screw settles on the maxilla. The mesh element size was specified as 1.3 mm on the contact surface of the sphenoid bone, 1 mm on the contact surface of the maxilla, and 0.8 mm on the first molar.

To enhance the precision of the analysis, the miniscrews of the expansion appliance and the threads of the miniscrew at their insertion points into the maxillary bone were defined with a mesh size of 0.1 mm (Fig. 1).

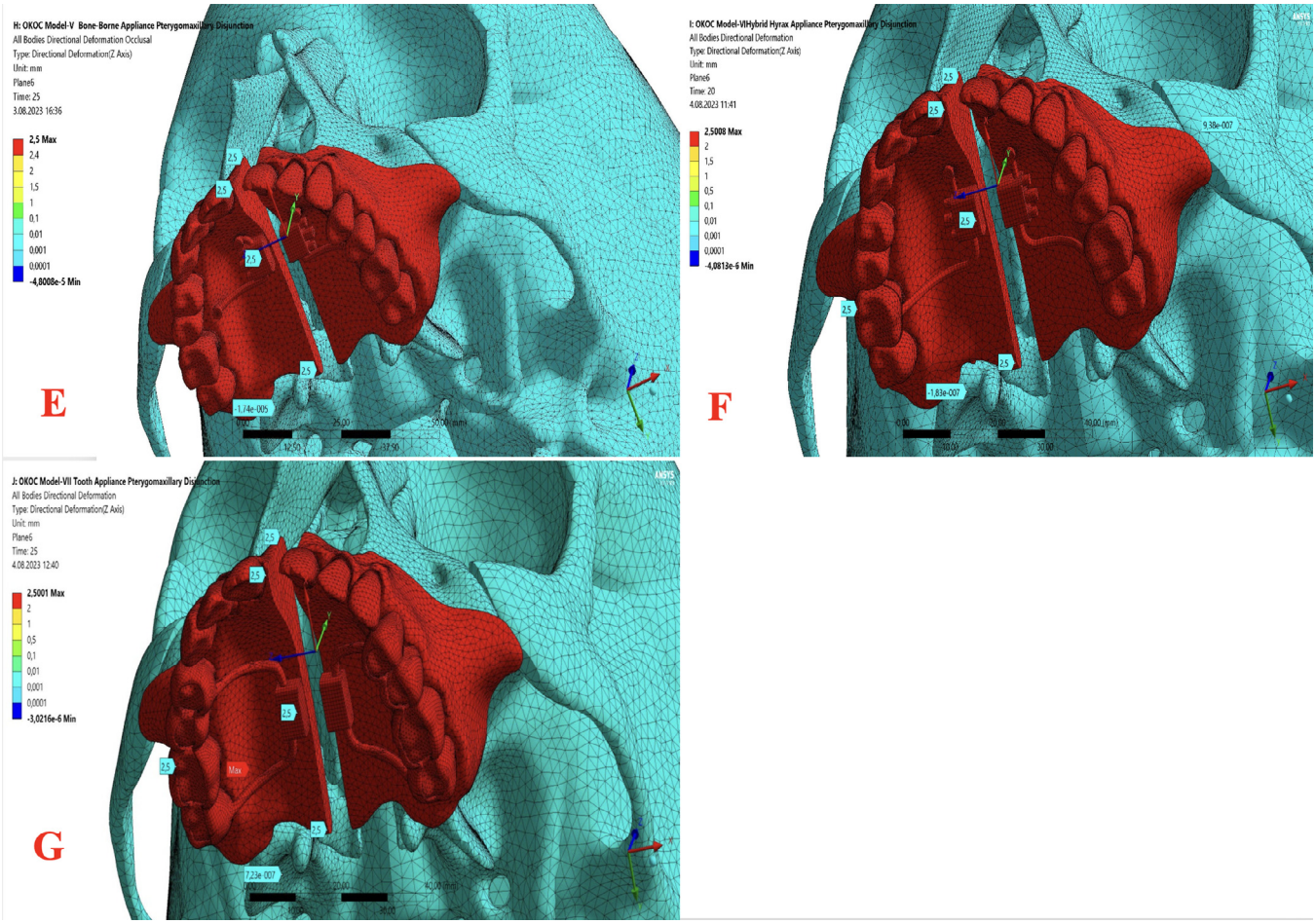


Fig. 3. Continued.

3. Results

3.1. Amount of displacement

This study's null hypothesis was rejected because there is a difference in the effects of different types of expansion appliances and various surgical techniques on maxillary expansion. In all models without PMD, except for Model I, the greatest amount of displacement occurred at the central incisors' level, and the transverse displacement of the incisors was greater than that of the posterior teeth. The largest transverse displacement in the central incisors was similar in Model II (3.50 mm), Model IV (3.34 mm) and Model III (3.31 mm), while 3.24 mm was measured in Model I, respectively. The minimum displacement value of 2.50 mm was found equal in Models V, VI and VII (Table 4). In these models, the transverse displacement was uniform across all teeth (Table 4, Fig. 3 and Videos 1–7).

The largest displacement value in the ANS was measured for Model-II (2.95 mm), Model-III (2.71 mm), Model V, VI, VII (2.50 mm), Model IV (2.15 mm), respectively; the smallest displacement was found (1.78 mm) for the Model I (Table 4). In the PNS, the highest displacement value in transverse direction was measured in Models V, VI, VII, (2,50 mm), and the lowest in Model III (0,79 mm) (Table 4, Fig. 3 and Videos 1–7).

In models without PMD, there was an increase in displacement along the z-axis from the second molar to the central incisor, whereas in the models with PMD, an equal amount of displacement was found in all teeth. In all models, the amount of displacement along the z-axis was greater in the medial pterygoid plate, than in the lateral pterygoid plate. The largest displacement for the z-axis of the medial pterygoid plate was measured in Model I (0.80 mm), while the smallest displacement was found in models with PMD (Models V, VI, VII). When the amount of displacement measured at the ANS and PNS points of the models without PMD was examined, a "V-shaped" expansion pattern was observed in the maxilla and this pattern was more pronounced in Model-II and Model-III. In the models with PMD, a parallel expansion pattern was observed in the maxilla (Fig. 3 and Videos 1–7).

3.2. Stress distribution

The highest elemental von Mises stress value was observed in Model I (Table 5). In models with PMD, the stress value was nearly zero at all anatomical points. Among the measured anatomical regions, the highest elemental von Mises stress values were found at the miniscrew insertion areas in Model I (329 MPa) and Model III (252 MPa), and at the medial pterygoid plate in Model II (175 MPa) and Model IV (113 MPa). The lowest elemental von Mises stress value measured at the miniscrew area was found in Model II (156 MPa) (Table 5, Fig. 4, 5 and Videos 1–7). In Model I (excluding the medial and lateral pterygoid plates), stress values measured in many anatomical areas were significantly higher compared to other models. The elemental von Mises stress value measured at the ANS was lowest in Model IV (0.04 MPa) and at PNS, the elemental von Mises stress

Table 5
The mean elemental stress (von Mises stress and first principal stress) distribution of the evaluated structures after 5 mm of the maxillary expander activation.

Anatomic structure	Model-I		Model-II		Model-III		Model-IV	
	Von Mises Stress (MPa)	First Principal Stress (MPa)	Von Mises Stress (MPa)	First Principal Stress (MPa)	Von Mises Stress (MPa)	First Principal Stress (MPa)	Von Mises Stress (MPa)	First Principal Stress (MPa)
Frontomaxillary suture	100	90.7	7.85	9.08	2.95	1.16	2.1	1.73
Zygomaticomaxillary suture	242.5	11.8	35.6	2.09	8.47	0.90	81.4	0.88
Frontozygomatic suture	180.9	8.02	16.7	-0.47	7.87	0.26	14.2	1.12
Zygomatic arch	159.5	40	6.36	0.28	7.62	0.44	8.84	4.96
Nasal frontal suture	169.5	157	14.3	17	10.85	13.8	7.86	7.27
Medial pterygoid plate	75.02	8.21	175	97.6	156.9	92.7	113	67.8
Lateral pterygoid plate	69.66	12.2	142	13.4	92.01	10.8	73.9	11.7
Maxillary tuberosity	14.38	4.54	16.7	12.5	5.18	4.47	12.7	11.5
Posterior nasal spine	10.8	6.88	1.92	0.33	0.64	0.24	0.98	0.07
Anterior nasal spine	15.7	9.54	0.13	0.05	1.29	0.10	0.04	0.04
Miniscrew region	329.6	289	156	111	252.8	239	-	-
1.Molar Tooth	3.095	5.8	0.06	0.05	126.6	5.49	1.95	0.37

Anatomic structure	Model-V		Model-VI		Model-VII	
	Von Mises Stress (MPa)	First Principal Stress (MPa)	Von Mises Stress (MPa)	First Principal Stress (MPa)	Von Mises Stress (MPa)	First Principal Stress (MPa)
Frontomaxillary suture	4.53e-5	-1.28e-6	1.09e-3	-1.47e-4	1.63e-4	-1.71e-6
Zygomaticomaxillary suture	1.31e-4	3.32e-5	2.10e-4	1.14e-3	4.06e-4	2.63e-6
Frontozygomatic suture	5.80e-5	-5.34e-6	5.55e-4	-4.22e-6	2.34e-4	-6.05e-6
Zygomatic arch	1.28e-4	3.93e-6	1.61e-3	2.63e-4	2.76e-4	4.60e-5
Nasal frontal suture	8.80e-5	-2.49e-5	2.70e-3	-4.76e-4	3.73e-4	-3.49e-5
Medial pterygoid plate	2.50e-4	1.35e-4	1.27e-2	5.64e-3	4.01e-4	4.84e-4
Lateral pterygoid plate	3.25e-4	1.48e-4	3.18e-2	1.79e-2	8.69e-4	6.71e-4
Maxillary tuberosity	4.36e-4	2.59e-4	2.10e-5	4.14e-6	2.67e-4	4.58e-5
Posterior nasal spine	8.70e-5	4.36e-5	6.45e-6	3.52e-6	1.32e-5	1.31e-5
Anterior nasal spine	2.67e-5	2.11e-6	1.19e-7	4.48e-8	1.61e-6	1.54e-6
Miniscrew region	2.06e-2	1.70e-2	2.79e-4	1.42e-4	-	-
1.Molar Tooth	5.03e-2	4.80e-2	3.34e-8	2.39e-8	1.81e-4	1.14e-4

Obs.: Positive (+) values indicate compression stress and negative (−) values indicate tensile stress; MPa=megapascal. 'e': Exponential. 'e' signifies the representation of a number as a base raised to a power/exponent. 10 to the power is expressed as a negative or positive (-/+) number.

value was lowest in Model III (0.64 MPa) (Table 5, Fig. 4 and Videos 1−7).

The maximum elemental stress values on the probe scale, showing stress distribution, were identified as exceedingly high. Specifically, for Models I, III, II, and IV, stress values reached 1016 MPa, 729 MPa, 472 MPa, and 388 MPa, respectively. Detailed analysis of the figures, particularly the regions shown in red representing maximum stress, unveiled concentration primarily at nodes and a limited number of elements within the volume. This concentration arises due to the occurrence of singularity errors (Fig. 4A, B, C, D).

The highest elemental von Mises stress in the first molar was observed in Model III (126.6 MPa), while the lowest elemental von Mises stress was recorded in the Model VI (3.34e-8 MPa) (Table 5, Fig. 4C,F).

In the maxillary tuber region, the highest elemental von Mises stress was observed in the Model II (16.7 MPa) and the lowest elemental von Mises stress was observed in the Model VI (2.10e-5 MPa) (Table 5, Fig. 4B,F).

4. Discussion

Based on the results obtained from this FEA, Model V, VI, and VII were identified as the optimal choices for clinical application, as these models exhibited reduced stress levels when analyzed using von Mises stress analysis. When PMD is performed, stress levels on craniofacial and maxillofacial structures are negligible, and the type of the expansion appliance has minimal effect.

In this investigation, the miniscrews of the expansion appliance were modeled with miniscrew threads to closely simulate clinical conditions. Notably, stress values of the miniscrew thread region, a parameter not precisely measured in prior studies, were a focus of this study. For a more accurate simulation of the clinical scenario, a symmetrical model was employed, simulating a total widening of 5 mm expansion (equivalent to 20 activations of the expander's screw). This approach aimed to capture the dynamic changes over time (with a total duration of 20 s) in a more realistic manner. This study adopted a nonlinear analysis method, employing three theories, to evaluate the impact of the expansion appliance on craniofacial and maxillofacial structures. Specially, transient structural analysis, known as dynamic analysis, was utilized. This method allowed for an exploration of the dynamic response, encompassing factors such as displacement, strain, stress, and forces, as the structure underwent changes influenced by time-varying transient loads [18].

Correcting skeletal transverse maxillary deficiency through maxillary expansion yields favorable functional and aesthetic outcomes [19]. In adult patients, maxillary expansion without surgical assistance may lead to dentoalveolar tipping and subsequent periodontal problems. Thus, SARPE has emerged as an alternative to prevent these side effects [20]. SARPE involves a Le Fort I osteotomy, performed under general anesthesia, without downward fracturing of the maxilla. Additionally, a midpalatal osteotomy is carried out [21].

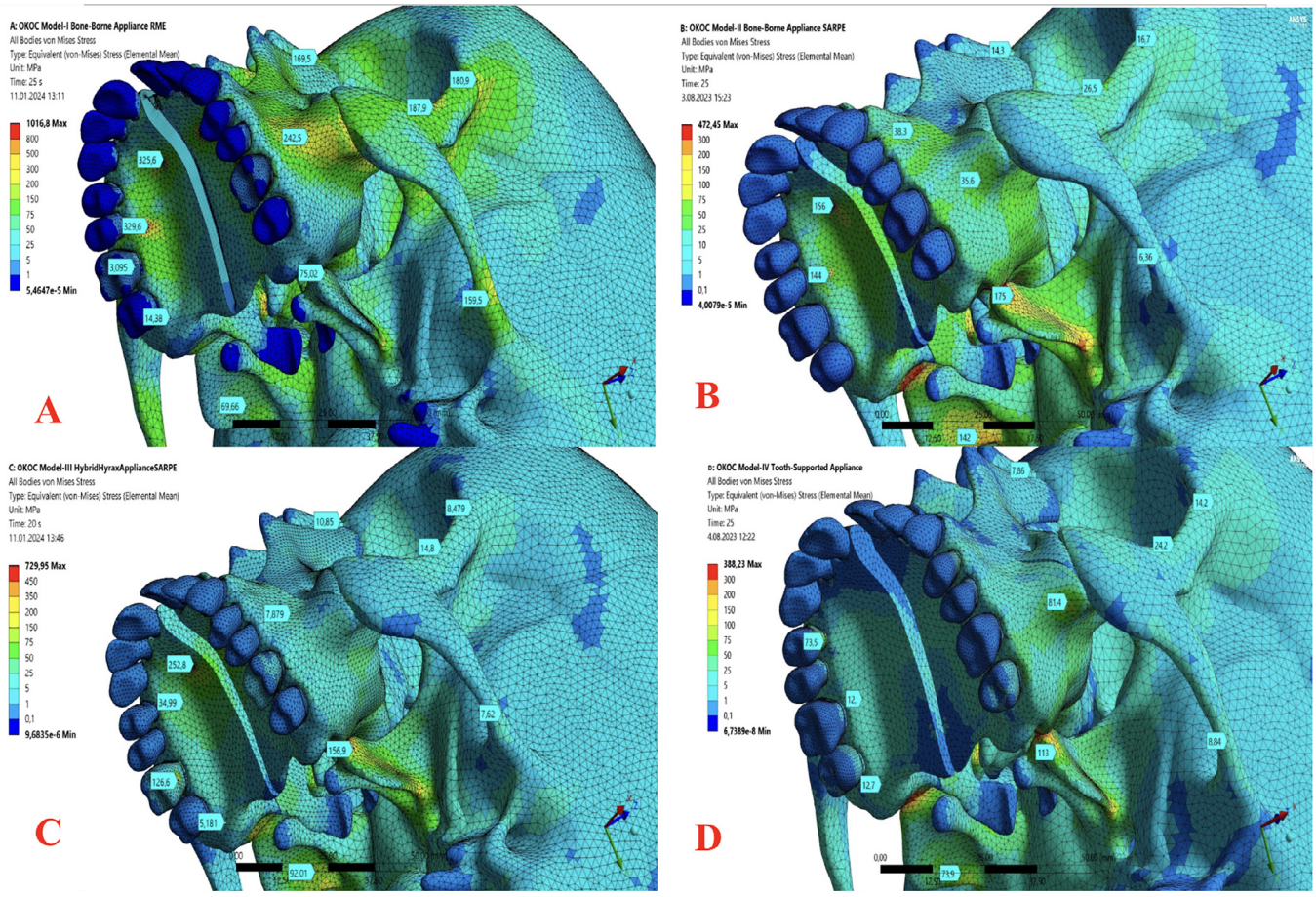


Fig. 4. **A,** Model I; **B,** Model II; **C,** Model III; **D,** Model IV; **E,** Model V; **F,** Model VI; **G,** Model VII; displaying the elemental von Mises stress value in MPa within the craniofacial and maxillofacial structures (occlusal perspective).

During the osteotomy procedure, a crucial decision arises regarding the necessity of performing PMD, involving the separation of the pterygoid plates from the maxilla. This delicate step is usually carried out with the surgeon's non-dominant hand providing support, while the dominant hand executes the osteotomy. Utilizing a curved chisel, the technique emphasizes careful attention to vascular structures in the posterior maxilla. The preservation of these structures is vital to reduce surgical bleeding and minimize postoperative risks, such as hemorrhage and avascular maxillary necrosis [22].

The literature lacks a consensus on the necessity and stability of PMD. A systematic review and meta-analysis revealed a lack of clear consensus in the literature regarding the necessity of PMD in SARPE [6]. Furthermore, uncertainties persist about whether PMD exerts different effects in correcting posterior versus anterior transverse discrepancies. Some surgeons caution against separating the pterygoid processes to avoid potential damage to the pterygoid plexus [21]. To establish precise indications for PMD and determine its necessity, a comprehensive evaluation of the procedure's outcomes is essential. Shi et al. [23] observed that displacements predominantly occurred in the transverse plane, especially following paramedian osteotomy combined with PMD. In cases without surgical intervention, they noted greater separation in the anterior segment of the midpalatal suture compared to the posterior segment. These findings align with Akkaya et al.'s [24] results, attributing the difference to higher resistance in the posterior maxillary region. However, the current study demonstrated reduced resistance in the posterior maxillary region, resulting in higher expansion in the posterior segment of the midpalatal suture, particularly in models with PMD. In this study, a greater amount of separation between centrals were observed in models without PMD compared to models with PMD. Surgeons performing SARPE should not perceive reduced separation between centrals as a failure. Such outcomes may be linked to different expansion patterns of the maxilla associated with each surgical technique [15]. An expansion pattern resembling a V-shape was observed in models without PMD. Conversely, in models with PMD, a parallel expansion pattern was observed in the maxilla. Similar to our results, a clinical study found that both SARPE with and without PMD proved to be effective in treating transverse maxillary deficiency [25]. Although no substantial differences were observed between the two groups, it appears that PMD contributes to greater expansion in the posterior palatal region, resulting in less molar tipping and a tendency toward a parallel opening along the medial palatal suture. Conversely, the absence of PMD may favor greater expansion of posterior teeth and a V-shaped opening from the midpalatal suture. In the anterior region, both methods demonstrated relative equality, with a slight inclination towards greater alveolar expansion when PMD is not performed [26].

Möhlenrich et al. [13] claimed that the controversial effect of PMD in SARPE becomes less significant when considering subsequent orthodontic treatment. Orthodontic treatment is likely to compensate for minor dentoalveolar differences resulting from both surgical techniques. Consequently, SARPE can be performed without PMD to minimize the risk of major surgical complications, although such complications are rare. Zandi et al. [25] observed comparable

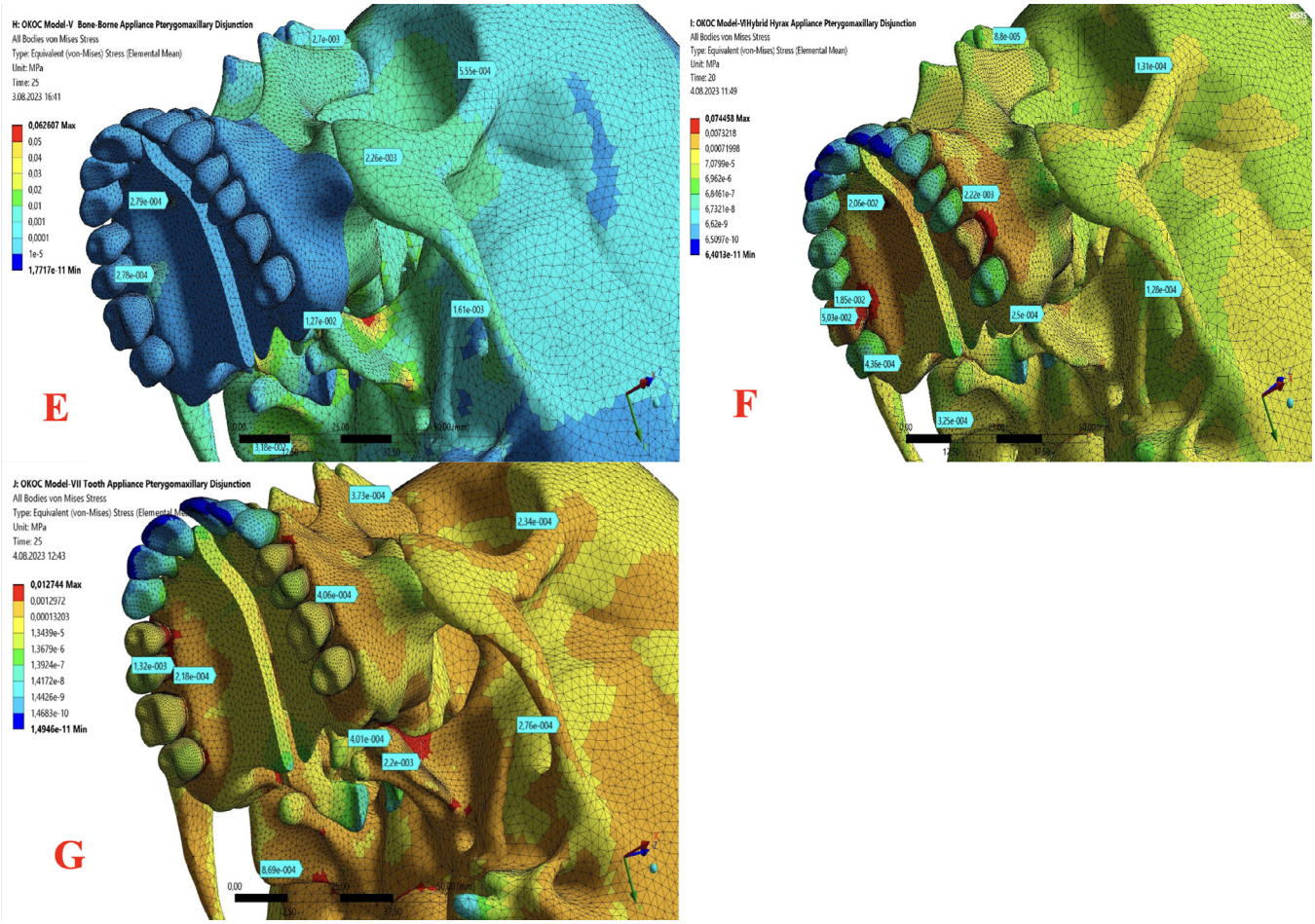


Fig. 4. Continued.

patterns of expansion in both the anterior and posterior aspects of the maxilla, regardless of whether PMD was performed. No notable disparities were identified in the extent or configuration of maxillary expansion between these two groups. Given the reduced likelihood of perioperative complications and the favorable surgical outcomes, it is recommended to consider SARPE without PMD as the preferred approach for addressing transverse maxillary deficiencies. Holberg et al. [12] indicated the importance of preventing the excessive stresses on cranial base during rapid maxillary expansion in adult patients to avoid undesirable side effects. One viable approach to reduce stress in the vicinity of the cranial base involves the surgical separation of the PMD. In the current study, it is recommended to separate the pterygoid plates due to higher levels of stress observed in cranial sutures in models without PMD compared to models with PMD. The highest stress values in the medial and lateral pterygoid plates were observed in Models II, III, and IV, respectively. PMD resulted in a notable reduction in stress values within the craniofacial structures. Additionally, a parallel expansion pattern was evident in the anteroposterior plane of the maxilla. It is reasonable to anticipate that the reduction in stress within the craniofacial and maxillofacial structures will contribute to a decrease in the likelihood of relapse.

Koç et al. [15] observed a V-shaped expansion pattern of the maxilla in their FEA models without PMD. The displacement and stress values on craniofacial structures in our study closely resemble those observed in models without PMD. In another FEA study, stress values were measured to be nearly zero in all sutural regions in models with PMD, and a parallel opening pattern of the maxilla was observed, similar to the current study [14]. Models without PMD exhibited high stress values in the miniscrew region and medial pterygoid region. In our study, models with PMD were compared with different types of expansion devices, yielding similar results.

When the surgical technique and the type of expansion appliance are altered, the stress values and displacement amounts on craniofacial structures can vary. This study adds a distinctive dimension to the evaluation of various expansion appliances in SARPE with PMD.

MARPE, a non-surgical method for expansion, has been advocated to enhance force distribution on the maxilla and its surrounding structures. MARPE aims to improve skeletal effect while minimizing the risk of dental tipping, consequently contributing to maintenance of the health of gingiva and teeth [27,28]. In a recent study involving 69 young adults treated with MARPE, a notable success rate of 86.96 % was reported [29]. Only nine cases did not achieve the desired midpalatal suture separation and they concluded that MARPE could be considered a viable non-surgical alternative for maxillary expansion. The current treatment approach suggests that both procedures can be used based on appropriate indications. However, this decision should be recommended after careful evaluation of periodontal condition, severity of the maxillary deficiency, and surgical risks. Therefore, ongoing research in this area is warranted.

Although MARPE appliances have been designed to enhance the orthopedic impact of maxillary expansion, studies comparing bone-borne and tooth-borne expanders have shown controversial results. Lin et al. [30] reported greater skeletal expansion with bone-borne appliances, while Lagravère et al. [31] found that both types of

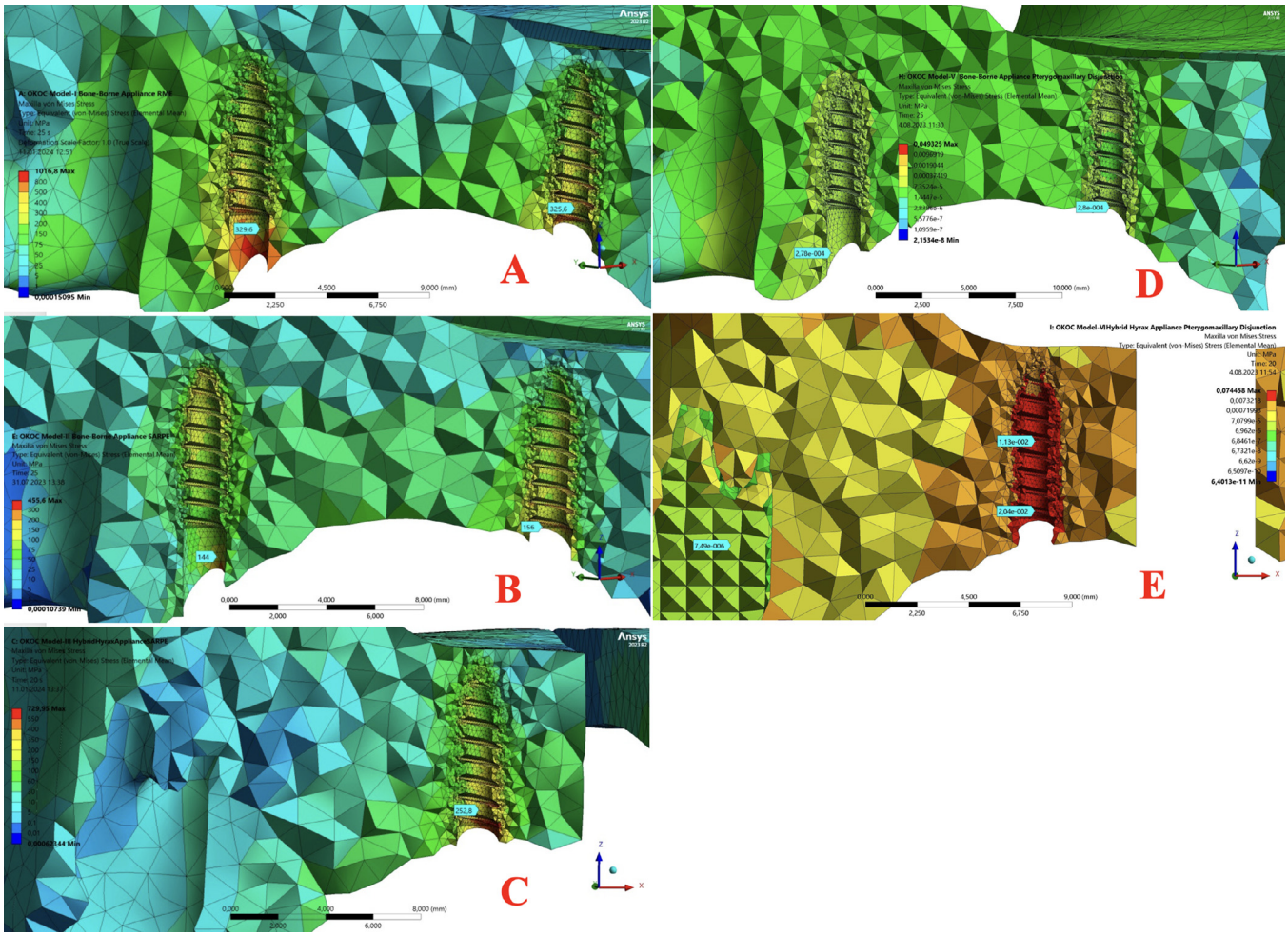


Fig. 5. **A,** Model I; **B,** Model II; **C,** Model III; **D,** Model V; **E,** Model VII; showing elemental von Mises stress values measured at the miniscrew areas.

expanders produced comparable skeletal effects. Cantarella et al. [32] demonstrated that MARPE effectively separated the midpalatal suture in late adolescents . This separation observed at ANS (4.8 mm) was approximately 90 % of that at PNS (4.3 mm), resulting in a nearly parallel expansion of the suture. The study suggested that the pterygopalatine suture can be separated with MARPE in late adolescents, without surgical assistance. MARPE managed to separate the lower part of the pterygopalatine suture in 53 % of cases by disengaging the pyramidal process of the palatine bone from the pterygoid notch of the sphenoid bone's pterygoid process.

Some studies advocated that MARPE alone is sufficient instead of SARPE [33]. However, it is important to note that MARPE is not without its challenges, particularly concerning stress levels in suture regions, which can lead to complications. Yoon et al. [34] found that common complications with MARPE include inflammation, pain, appliance breakage or distortion, and asymmetrical expansion. In their study, 47.8 % of patients exhibited asymmetric expansion. This percentage is notably higher compared to another study, which reported an asymmetric expansion rate of 30.3 % [35]. In contrast, studies assessing expansion in SARPE found that only 3.3 % to 13.3 % of patients experienced asymmetric or insufficient expansion [36]. These findings underscore the importance of carefully considering the potential complications associated with MARPE, particularly in terms of asymmetrical expansion.

In the current study's MARPE model, higher levels of elemental von Mises stress were observed in the miniscrew regions and sutural areas compared to all other models. SARPE models with PMD exhibited the lowest stress levels. Notably, the MARPE model showed a transverse upward rotation of the maxilla. SARPE models without PMD demonstrated reduced rotational movement compared to the MARPE model and exhibited a V shaped expansion pattern. Among all models, SARPE models with PMD demonstrated the most parallel expansion pattern. Considering the findings of this FEA study, SARPE with PMD is recommended for achieving a parallel expansion with lower stress levels.

The present study stands out from recent FEA studies by incorporating miniscrew grooves into the model design [14-16]. Additionally, this investigation evaluates the influence of the midpalatal suture on expansion. Stress values were notably higher in the mini screw region of the MARPE model, potentially leading to microdamage in bone. A potential outcome that may arise is associated with stresses exceeding the bone's yield strength. Without adequate remodeling observed during the expansion period, there exists a risk of miniscrew loss. Especially in adult patients with suture maturation and high bone density, elevated stress values may result in miniscrew loss in MARPE treatment.

When the models of this study were evaluated, the MARPE model demonstrated the highest stress values on the craniofacial structure, especially in the miniscrew region. The region presenting the greatest resistance to maxillary expansion in the MARPE model was identified as the zygomaticomaxillary suture. Evaluation based on the material property (modulus of elasticity) assigned to the midpalatal suture revealed no notable effect on expansion resistance. In models without PMD, the region displaying the highest resistance was identified as the medial pterygoid plate and miniscrew regions.

4.1. Limitations

Post-expansion relapse, bone remodeling, and the effects of soft tissues, muscles, and chewing forces were not included in this FEA study. Clinical studies are needed to investigate these effects.

The maximum average elemental stress values arise from singularity errors. Singularity errors have been mentioned in previous FEA studies [14-16]. However, the maximum stress values resulting from singularity errors in this analysis did not impact the results.

5. Conclusions

5.1. Within the limitations of this FEA study;

1) The MARPE model demonstrated a transverse upward rotation of the maxilla. In SARPE models without PMD, a V-shaped expansion pattern was observed in the maxilla. In contrast, models with PMD exhibited a parallel expansion pattern in the maxilla. Various designs of expanders resulted in different stress levels in SARPE models with PMD.
2) In the MARPE model, higher levels of stress were noted in the miniscrew regions and sutural areas compared to all other models. SARPE models with PMD demonstrated nearly zero stress levels at all anatomical points.
3) SARPE with PMD is characterized by lower stress levels in craniofacial structures, decreasing the probability of insufficient expansion.
4) When performing MARPE or SARPE for maxillary expansion, clinicians should pay attention to potential complications, stress distribution in different regions, resistance points in the craniofacial structure, and the need for further research to better understand the effects of these techniques.

Declaration of competing interest

The authors declare that they have no known competing financial interests or personal relationships that could have appeared to influence the work reported in this paper.

CRediT authorship contribution statement

Ece Mersan Ateş: Writing – original draft, Investigation, Funding acquisition, Data curation. **Hande Pamukçu:** Writing – review & editing, Supervision, Methodology, Funding acquisition, Conceptualization. **Osman Koç:** Writing – review & editing, Software, Formal analysis, Data curation, Conceptualization. **Nur Altınparmak:** Writing – review & editing, Supervision, Methodology, Conceptualization.

Supplementary materials

Supplementary material associated with this article can be found, in the online version, at doi:10.1016/j.jormas.2024.101936.

References

[1] Haas AJ. Palatal expansion: just the beginning of dentofacial orthopedics. Am J Orthod 1970;57(3):219–55. doi: 10.1016/0002-9416(70)90241-1.
[2] Harzer W, Schneider M, Gedrange T, Tausche E. Direct bone placement of the hyrax fixation screw for surgically assisted rapid palatal expansion (SARPE). J Oral Maxillofac Surg 2006;64(8):1313–7. doi: 10.1016/j.joms.2005.11.061.
[3] Kennedy 3rd JW, Bell WH, Kimbrough OL, James WB. Osteotomy as an adjunct to rapid maxillary expansion. Am J Orthod 1976;70(2):123–37. doi: 10.1016/s0002-9416(76)90313-4.
[4] Ferraro-Bezerra M, Tavares RN, de Medeiros JR, Nogueira AS, Avelar RL. Studart Soares EC. Effects of pterygomaxillary separation on skeletal and dental changes after surgically assisted rapid maxillary expansion: a single-center, double-blind, randomized clinical trial. J Oral Maxillofac Surg 2018;76(4):844–53. doi: 10.1016/j.joms.2017.08.032.
[5] Carvalho PHA, Moura LB, Trento GS, Holzinger D, Gabrielli MAC, Gabrielli MFR, Pereira Filho VA. Surgically assisted rapid maxillary expansion: a systematic review of complications. Int J Oral Maxillofac Surg 2020;49(3):325–32. doi: 10.1016/j.ijom.2019.08.011.
[6] Hamedi Sangsari A, Sadr-Eshkevari P, Al-Dam A, Friedrich RE, Freymiller E, Rashad A. Surgically assisted rapid palatomaxillary expansion with or without pterygomaxillary disjunction: a systematic review and meta-analysis. J Oral Maxillofac Surg 2016;74(2):338–48. doi: 10.1016/j.joms.2015.06.161.
[7] Wilmes B, Drescher D. A miniscrew system with interchangeable abutments. J Clin Orthod 2008;42(10):574–80 quiz 595. PMID: 19075372.
[8] Choi JY, Choo H, Oh SH, Park JH, Chung KR, Kim SH. Finite element analysis of C-expanders with different vertical vectors of anchor screws. Am J Orthod Dentofacial Orthop 2021;159(6):799–807. doi: 10.1016/j.ajodo.2020.02.024.
[9] Kapetanović A, Theodorou CI, Bergé SJ, Schols JGJH, Xi T. Efficacy of miniscrew-assisted rapid palatal expansion (MARPE) in late adolescents and adults: a systematic review and meta-analysis. Eur J Orthod 2021;43(3):313–23. doi: 10.1093/ejo/cjab005.
[10] Kapetanović A, Odrosslij BMMJ, Baan F, Bergé SJ, Noverraz RRM, Schols JGJH, Xi T. Efficacy of miniscrew-assisted rapid palatal expansion (MARPE) in late adolescents and adults with the dutch maxillary expansion device: a prospective clinical cohort study. Clin Oral Invest 2022;26(10):6253–63. doi: 10.1007/s00784-022-04577-9.
[11] Gautam P, Valiathan A, Adhikari R. Stress and displacement patterns in the craniofacial skeleton with rapid maxillary expansion: a finite element method study. Am J Orthod Dentofac. Orthop 2007;132(1) 5.e1-11. doi: 10.1016/j.ajodo.2006.09.044.
[12] Holberg C, Steinhäuser S, Rudzki I. Surgically assisted rapid maxillary expansion: midfacial and cranial stress distribution. Am J Orthod Dentofacial Orthop 2007;132(6):776–82. doi: 10.1016/j.ajodo.2005.12.036.
[13] Möhlhenrich SC, Heeg J, Raith S, Kniha K, Hölzle F, Wolf M, Fritz U, Modabber A. Effect of the pterygomaxillary disjunction on surgically assisted rapid palatal expansion in context of orthodontic treatment. Oral Surg Oral Med Oral Pathol Oral Radiol 2020;130(3):241–51. doi: 10.1016/j.oooo.2020.03.048.
[14] Koç O, Jacob HB. Surgically assisted rapid palatal expansion: is the pterygomaxillary disjunction necessary? A finite element study. Semin Orthod 2022;28(3):227–42. doi: 10.1053/j.sodo.2022.10.017.
[15] Koç O, Pamukçu H, Kocabalkan AA. Comparison of 3 different bone-borne type expansion appliances used in surgically-assisted rapid palatal expansion: a finite element analysis. Am J Orthod Dentofacial Orthop 2023;163(3):e23–33. doi: 10.1016/j.ajodo.2022.12.001.
[16] Koç O, Bolat Gumus E. Effects of different distractor positions on the formation of expansion, stress and displacement patterns in surgically assisted rapid maxillary expansion without pterygomaxillary disjunction: a finite element analysis study. Comput Methods Biomech Biomed Engin 2024;27(1):56–66. doi: 10.1080/10255842.2023.2170712.
[17] Life science database archive: BodyParts3D., 2021 Available at: https://dbarchive.biosciencedbc.jp/jp/bodyparts3d/desc.html.
[18] Bi Z. Finite element analysis applications a systematic and practical approach. 1st Edition Cambridge, Massachusetts: Academic Press; 2018.
[19] Vandersea BA, Ruvo AT, Frost DE. Maxillary transverse deficiency - surgical alternatives to management. Oral Maxillofac Surg Clin North Am 2007;19(3):351–68 vi. doi: 10.1016/j.coms.2007.04.007.
[20] Chang JY, McNamara Jr JA, Herberger TA. A longitudinal study of skeletal side effects induced by rapid maxillary expansion. Am J Orthod Dentofacial Orthop 1997;112(3):330–7. doi: 10.1016/S0889-5406(97)70264-6.
[21] Kanazawa T, Kuroyanagi N, Miyachi H, Ochiai S, Kamiya N, Nagao T, Shimozato K. Factors predictive of pterygoid process fractures after pterygomaxillary separation without using an osteotome in Le Fort I osteotomy. Oral Surg Oral Med Oral Pathol Oral Radiol 2013;115(3):310–8. doi: 10.1016/j.oooo.2012.04.020.
[22] Koudstaal MJ, Poort LJ, van der Wal KG, Wolvius EB, Prahl-Andersen B, Schulten AJ. Surgically assisted rapid maxillary expansion (SARME): a review of the literature. Int J Oral Maxillofac Surg 2005;34(7):709–14. doi: 10.1016/j.ijom.2005.04.025.
[23] Shi Y, Zhu CN, Xie Z. Displacement and stress distribution of the maxilla under different surgical conditions in three typical models with bone-borne distraction: a three-dimensional finite element analysis. J Orofac Orthop 2020;81(6):385–95. doi: 10.1007/s00056-020-00251-5.
[24] Akkaya S, Lorenzon S, Uçem TT. Comparison of dental arch and arch perimeter changes between bonded rapid and slow maxillary expansion procedures. Eur J Orthod 1998;20(3):255–61. doi: 10.1093/ejo/20.3.255.
[25] Zandi M, Miresmaeili A, Heidari A, Lamei A. The necessity of pterygomaxillary disjunction in surgically assisted rapid maxillary expansion: a short-term, double-blind, historical controlled clinical trial. J Craniomaxillofac Surg 2016;44(9):1181–6. doi: 10.1016/j.jcms.2016.04.026.
[26] Chen KY, Yang CY, Fan CN, Kuo CS, Fan SZ, Chen YW. The effects of pterygomaxillary disjunction in surgically assisted rapid maxillary expansion: a systematic review and meta-analysis. Orthod Craniofac Res 2024. doi: 10.1111/ocr.12797.
[27] Garib DG, Navarro R, Francischone CE, Oltramari PV. Rapid maxillary expansion using palatal implants. J Clin Orthod 2008;42(11):665–71.
[28] Yılmaz A, Arman-Özçırpıcı A, Erken S. Polat-Özsoy Ö. Comparison of short-term effects of mini-implant-supported maxillary expansion appliance with two conventional expansion protocols. Eur J Orthod 2015;37(5):556–64. doi: 10.1093/ejo/cju094.
[29] Choi SH, Shi KK, Cha JY, Park YC, Lee KJ. Nonsurgical miniscrew-assisted rapid maxillary expansion results in acceptable stability in young adults. Angle Orthod 2016;86(5):713–20. doi: 10.2319/101415-689.1.

[30] Lin L, Ahn HW, Kim SJ, Moon SC, Kim SH, Nelson G. Tooth-borne vs bone-borne rapid maxillary expanders in late adolescence. Angle Orthod 2015;85(2):253–62. doi: 10.2319/030514-156.1.
[31] Lagravère MO, Carey J, Heo G, Toogood RW, Major PW. Transverse, vertical, and anteroposterior changes from bone-anchored maxillary expansion vs traditional rapid maxillary expansion: a randomized clinical trial. Am J Orthod Dentofacial Orthop 2010;137(3) 304.e1-12. doi: 10.1016/j.ajodo.2009.09.016.
[32] Cantarella D, Dominguez-Mompell R, Mallya SM, Moschik C, Pan HC, Miller J, Moon W. Changes in the midpalatal and pterygopalatine sutures induced by micro-implant-supported skeletal expander, analyzed with a novel 3D method based on CBCT imaging. Prog Orthod 2017;18(1):34. doi: 10.1186/s40510-017-0188-7.
[33] de Oliveira CB, Ayub P, Ledra IM, Murata WH, Suzuki SS, Ravelli DB, Santos-Pinto A. Microimplant assisted rapid palatal expansion vs surgically assisted rapid palatal expansion for maxillary transverse discrepancy treatment. Am J Orthod Dentofacial Orthop 2021;159(6):733–42. doi: 10.1016/j.ajodo.2020.03.024.
[34] Yoon A, Payne J, Suh H, Phi L, Chan A, Oh H. A retrospective analysis of the complications associated with miniscrew-assisted rapid palatal expansion. AJO-DO Clin Companion. 2022;2(5):423–30 1. doi: 10.1016/j.xaor.2022.08.001.
[35] Kim KA, Oh SH, Kim BH, Kim SJ. Asymmetric nasomaxillary expansion induced by tooth-bone-borne expander producing differential craniofacial changes. Orthod Craniofac Res 2019;22(4):296–303. doi: 10.1111/ocr.12320.
[36] Smeets M, Da Costa Senior O, Eman S, Politis C. A retrospective analysis of the complication rate after SARPE in 111 cases, and its relationship to patient age at surgery. J Craniomaxillofac Surg 2020;48(5):467–71. doi: 10.1016/j.jcms.2019.12.015.